Food web structure and intraguild predation affect ecosystem functioning in an established plankton model

A. E. Friederike Prowe [1*] Bei Su [2,3,4*] Jens C. Nejstgaard [5] Markus Schartau [1]

[1]GEOMAR Helmholtz Centre for Ocean Research Kiel, Kiel, Germany
[2]Institute of Marine Science and Technology, Shandong University, Qingdao, China
[3]Southern Marine Science and Engineering Guangdong Laboratory, Zhuhai, China
[4]School of Environmental Sciences, University of Liverpool, Liverpool, UK
[5]Leibniz Institute of Freshwater Ecology and Inland Fisheries (IGB), Stechlin, Germany

Abstract

Understanding how marine microbial food webs and their ecosystem functions are changing is crucial for projections of the future ocean. Often, simplified food web models are employed and their solutions are only evaluated against available observations of plankton biomass. With such an approach, it remains unclear how different underlying trophic interactions affect interpretations of plankton dynamics and functioning. Here, we quantitatively compare four hypothetical food webs to data from an existing mesocosm experiment using a refined version of the Minimum Microbial Food Web model. Food web representations range from separated food chains to complex food webs featuring additional trophic links including intraguild predation (IGP). Optimization against observations and taking into account model complexity ensures a fair comparison of the different food webs. Although the different optimized model food webs capture the observations similarly well, projected ecosystem functions differ depending on the underlying food web structure and the presence or absence of IGP. Mesh-like food webs dominated by the microbial loop yield higher recycling and net primary production (NPP) than models dominated by the classical diatom-copepod food chain. A high degree of microzooplankton IGP increases NPP and organic matter recycling, but decreases trophic transfer efficiency (TTE) to copepods. Copepod production, the trophic role of copepods, and TTE are more sensitive to initial biomass changes in chain-like than in complex food webs. Measurements resolving trophic interactions, in particular those quantifying IGP, remain essential to reduce model uncertainty and allow sound conclusions for ecosystem functioning in plankton ecosystems.

Marine ecosystems, particularly in the Arctic, are under pressure from rapidly progressing global climate change. Changes in ocean physics drive shifts in phytoplankton community composition (Li et al. 2009), seasonality (Søreide et al. 2010) and mesozooplankton biogeography (McGinty et al. 2021), with effects on biogeochemistry and important ecosystem functions like the vertical export of organic carbon to the deep ocean (Brun et al. 2019). Changes in the lower trophic levels (TLs) may drive reductions in fisheries production and other ecosystem services (Dobson et al. 2006). Future projections of primary production and net community production in response to changes in environmental conditions or fishing pressure require the use of reliable plankton ecosystem models. Typically, these models reduce diverse plankton trophic interactions to few equations resolving the apparently most important links between relevant groups. These presumably dominant trophic interactions then define the model's food web structure that is employed to simulate dynamics of the different plankton groups as biomass change over time. The food web structure of plankton and the number and type of trophic interactions are expected to affect ecosystem functions such as mesozooplankton production available to fish or carbon export (Steinberg and Landry 2017; Maar et al. 2018).

An established model with a simple trophic structure is the Minimum Microbial Food Web model (hereafter referred to as the Minimum model; Thingstad et al. 2007). Using this model, simulations of different mesocosm experiments have helped to unravel predominant dynamics and states of the marine pelagic microbial food web (Thingstad 2020). Larsen

*Correspondence: fprowe@geomar.de; bei.su@sdu.edu.cn

et al. (2015) adjusted the model's food web by adding a trophic link from diatoms to microzooplankton, here referred to as ciliates. Based on this addition, the model could explain data from the Polar Aquatic Microbial Ecology (PAME) mesocosm experiments and thereby resolve differences in microbial community responses due to variations in mesozooplankton abundance. From these existing analyses, it is not clear, however, whether the available biomass observations suffice to unambiguously identify the underlying trophic interactions that ultimately determine the food web structure.

One important trophic interaction in both natural plankton communities (Franzé and Modigh 2013) and mesocosm modeling (Su et al. 2018) is intraguild predation (IGP), which describes feeding interactions between consumers that share the same resources (Holt and Polis 1997). For copepods (Dufour et al. 2016) as well as for microzooplankton (*see* references in Franzé and Modigh 2013; Kuppardt-Kirmse and Chatzinotas 2020), in particular for dinoflagellates and ciliates (Diehl and Feissel 2001; Löder et al. 2014; Yang et al. 2021) and heterotrophic flagellates (Moustaka-Gouni et al. 2016) IGP has frequently been inferred, and high IGP rates of up to 79% of microzooplankton production have been demonstrated experimentally (Franzé and Modigh 2013).

In the present study, we investigate the role of trophic interactions, including IGP, for plankton dynamics over time and we analyze how the different resulting food web structures affect projections of ecosystem functions. We compare models with different food web structures that build on the Minimum model versions of Thingstad et al. (2007) and Larsen et al. (2015) and are individually fitted to observations of the PAME-I mesocosm experiment. In this way, we obtain different hypothetical explanations for the same observations. We use an optimization algorithm to objectively compare the fit of different model food webs to the observations. Different implications of these food webs for ecosystem functioning are revealed by quantifying net primary and secondary production, recycling, trophic transfer efficiency (TTE) and the maximum trophic level of copepods (TL_M), and by simulating model sensitivities to changes in initial biomass.

Methods

As testbed for comparing different food webs we use observations of the mesocosm experiment PAME-I conducted in Kongsfjorden in Svalbard and previously analyzed with the Minimum model (Larsen et al. 2015). The original model simulates phosphate (P), bacteria (B), autotrophic (A) and heterotrophic (H) nanoflagellates (also referred to as ANFs and HNFs, respectively), diatoms (D), ciliates (C), and mesozooplankton (M), representing calanoid copepods as dominant group in the experiment, arranged in a double-pentagon food web (Supporting Information Fig. S1). Comparing different hypothetical food webs requires an objective and thus quantitative assessment of the best possible model representations of the observational data (metric). This is achieved by applying an optimization algorithm that minimizes the data-model misfit (cost function). The minima of the cost function values yield best (optimal) combinations of parameter values for each of the various model food webs, thereby providing best fits to the observations.

The original model equations of the Minimum model (Thingstad et al. 2007; Larsen et al. 2015) were coded in Matlab (Mathworks) based on the authors' original R Code. The pulsed additions of PO_4^{3-} at specific times during the mesocosm experiments are represented as continuous input flux as in Larsen et al. (2015). Further details on the model setup can be found in the Supporting Information. Two model refinements essential for model optimization are detailed below.

P accumulation

The original model was extended by an additional state variable UOP* (untraced organic phosphorus; Supporting Information Fig. S2), which represents the imbalance between the measured (inorganic and organic) phosphorus pool and the expected actual total phosphorus, assuming mass conservation within the mesocosms. Accordingly, the UOP* in the mesocosms is estimated from the difference of the documented PO_4^{3-} addition rate ($E_{P_i}t_i$) and the total P in observed variables (P_t; Supporting Information Eqs. S10, S11). In the model, UOP* is attributed to unassimilated fractions of grazing, in response to sloppy feeding, excretion and fecal pellet production (Supporting Information Eq. S12). UOP* is remineralized to PO_4^{3-} with rate R and may therefore contribute to regenerated production. Simulated UOP* is assessed against the observation-based estimates at times when all variables were measured. This approach proves essential for assuring identical constraints with respect to mass conservation for all model setups.

Initial values

The solutions of the original Minimum model (Thingstad et al. 2007; Larsen et al. 2015) rely on a steady-state assumption to calculate initial values for each variable. This implies that initial values differ for different combinations of parameter values. In order to separate effects of initial conditions and changes in parameter values on model performance, present model simulations start from fixed observed initial values for each variable. Sensitivities of the simulated dynamics to changes in initial conditions are assessed separately by creating an ensemble of 1000 random (independent and identically distributed) initial conditions, covering a range (upper and lower bounds) of ± 20% around the observed initial concentrations of P, B, A, D, H, C, and M. This variational range is proportioned to the mean of the relative (normalized) deviations between the initial conditions in Larsen et al. (2015) and our estimates (Supporting Information Table S2), which is

21%. The same ensemble of initial conditions is applied to all model configurations.

Food web configurations

Based on the above modifications, this study compares four basic food web configurations (Supporting Information Table S3):

1. *control*: The original Minimum model food web (Thingstad et al. 2007), without trophic link between diatoms and ciliates.

2. *d2c*: The food web of Larsen et al. (2015), with ciliates feeding on diatoms (the D – C link).

3. *ig*: The *control* food web with additional (intraguild) predation of ciliates on their own compartment.

4. *igd2c*: Combining food webs *ig* and *d2c,* allowing grazing of ciliates on diatoms and themselves.

A feeding link between diatoms and ciliates (Larsen et al. 2015) can be justified by the observation of small-celled diatoms in PAME-I that are within the prey size range of microzooplankton. Here, we keep the established name of the compartment, "ciliates (C)," to denote all larger microzooplankton in contrast to the smaller heterotrophic nanoflagellates (H), without excluding other "larger" microzooplankton such as dinoflagellates or rotifers. However, in the PAME studies, heterotrophic dinoflagellates and rotifers were not quantified, due to too small volumes analyzed.

During the experiments, two distinct size classes of ciliates were observed, either notably larger or smaller than $30\,\mu m$ in body size (Jens Nejstgaard, pers. obs.). As ciliates of $>30\,\mu m$ body size can feed on relatively large prey including other ciliates (Dolan and Coats 1991; Diehl and Feissel 2001; Vasseur and Fox 2009) and IGP for microzooplankton has been repeatedly reported (e.g., references in Franzé and Modigh 2013), we consider IGP as plausible trophic link in configuration *ig.*

Further food webs including a feeding threshold for mesozooplankton feeding on diatoms were tested alone and in combination, but yielded worse fits and did not change the findings from the configurations presented above (*see* Supporting Information for details).

The model configurations represent different levels of complexity in terms of numbers of parameters (Table 1; Supporting Information Tables S3, S4). Forcing parameters and the initial values remain fixed (Supporting Information Table S2). In preliminary optimizations the growth efficiency or yield values (Y_H, Y_C, Y_M) were always optimized to their

upper ($Y_H = Y_C = 0.4$) and lower ($Y_M = 0.1$) limits of physiologically reasonable values according to literature and expert knowledge, and these parameters are not optimized.

Model calibration and assessment

The optimization algorithm used is the Matlab version of the Covariance Matrix Adaptation Evolution Strategy algorithm (CMA-ES; Hansen and Ostermeier 2001). CMA-ES generates random combinations of values for the parameters to be optimized. For each combination, the model results are evaluated against the observational data, using a cost function that quantifies the model-data misfit. As preparation, the optimization setup was tested by treating model results of a reference solution as pseudo-data (identical twin data). This twin experiment allowed us to consolidate the optimizer's performance and introduce refinements, here including UOP* in the cost function. Sampling dates and respective observational uncertainties of the original data are considered and all parameter values that were used to generate the reference model results (pseudo-data) were identified by the optimization.

The cost function J is calculated as

$$J = \sum_{i=1}^{N_t} \sum_{j=1}^{N_y} \frac{\left(y_{ij} - \eta_{ij}(x)\right)^2}{\sigma_{ij}^2}, \qquad (1)$$

with observations y_{ij} for $y = P, B, A, D, H, C, M, UOP^*$ and model data η_{ij} at times $i = 1, \ldots, t$ of the observations. σ is taken as the measurement uncertainty of the observations y. Since observational errors are not reported in the original publication, values of σ are set to reflect minimal yet plausible observational error assumptions (e.g., a detection limit for PO_4^{3-}; Supporting Information Table S1). The identification of this cost function's minimum is tantamount to having found maximum likelihood parameter estimates for a given model.

Similar to Thingstad et al. (2007), this study attempts to identify a model configuration of minimum complexity that simulates the essential dynamics involved in the microbial food web. Accordingly, we apply the law of parsimony while testing model configurations of different complexity. The simpler models are nested subversions of the most complex model configuration, which allows us to assess the models' performances against each other. For the assessment we apply the *F*-score as a metric (Ward et al. 2013; Schartau et al. 2017,

Table 1. Cost function values *J*, *F*-score (Supporting Information Eq. S14) using the most complex model *igd2c* as reference, and threshold *F*-value of $\alpha = 0.05$ for food webs of different complexity (N_p number of optimized parameters).

Simulation	Food web	N_p	J	*F*-score	Threshold *F*
control	As used in Thingstad et al. (2007)	14	528.15	7.83	3.24
ig	C feeding on themselves (intraguild grazing)	15	454.20	8.51	4.01
d2c	As in Larsen et al. (2015) with C feeding on D	15	458.99	8.01	4.01
igd2c	Full model: C feeding on D and on themselves	16	376.78	—	—
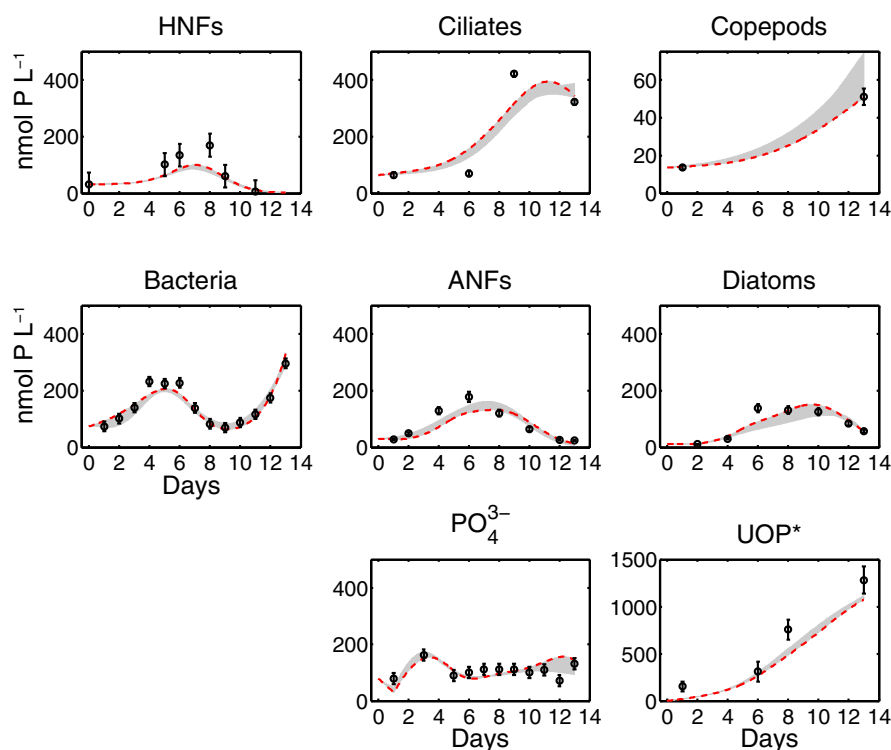
Fig. 1. Simulated dynamics of observed variables (circles) during PAME-I and estimated phosphorus accumulation (UOP*) for configuration *igd2c* with best fit to observations (red dashed line). Gray shading indicates the min–max envelope of the four simulations with different food webs (cf. Supporting Information Fig. S3 for individual simulations).

cf. Supporting Information). An *F*-score below or equal to a threshold value identifies the best and simplest (i.e., most parsimonious) model with comparable performance. The threshold values of *F* are computed for the $\alpha = 0.05$ confidence level.

Ecosystem functions

Several ecosystem functions are estimated from the model simulations. Net primary production (NPP) is calculated from PO_4^{3-} uptake of A and D using a fixed molar C : P ratio of 106. Net secondary production (NSP) of H, C, and M is calculated from the assimilated part of ingestion (*YI*, with yield values Y_H, Y_C, and Y_M) using a fixed molar C : P ratio of 50 (Larsen et al. 2015). TTE from autotrophic production to mesozooplankton (here copepods) is estimated as TTE = $Y_M I$/NPP (Supporting Information Eq. S15). The TL of mesozooplankton is estimated from partial ingestion of diatoms and ciliates as $TL_M = 1 + TL_D$ ingestion (D)/total ingestion + TL_C ingestion (C)/total mesozooplankton ingestion, assuming $TL_D = 1$ for diatoms (D) and taking into account a variable TL (TL_C) of ciliates (C; Supporting Information Eqs. S16, S17).

Results

The PAME-I experiment
The best model

All optimized food webs simulate the observational data well (Fig. 1), notably improving earlier projections (Larsen

et al. 2015, their fig. 8). According to the visual impression, the model performances appear to be similar (no more than 40% deviation from the lowest cost function value of the most complex model *igd2c*, *see* Table 1). A more notable spread in simulated dynamics is only evident for copepods (Fig. 1; Supporting Information Fig. S3). Using the most complex *igd2c* model as reference, the *F* score for any simpler model does not fall below the respective threshold (Table 1). In particular, models with each inherent feeding interaction, the D – C feeding link and IGP, separately do not provide fits as good (*F*-score exceeding threshold).

Food web structure

Despite reproducing the biomass observations similarly well, the model configurations imply different underlying food webs and dominant pathways. The four models fall within two categories indicated by the strength of the ciliate-copepod interaction. In the *igd2c* and *d2c* food webs, copepods feed on ciliates, while in the *control* and *ig* food webs, copepods almost completely rely on diatoms as food source (Fig. 2; cf. Supporting Information Table S5 for the optimized parameter values). The latter model solutions embody the "classic" grazing food chain from diatoms to herbivorous copepods, in the following referred to as *chain-like* food webs. In contrast, the *igd2c* and *d2c* solutions are more *mesh-like*, with copepods also feeding on ciliates. This distinction between *chain-like*
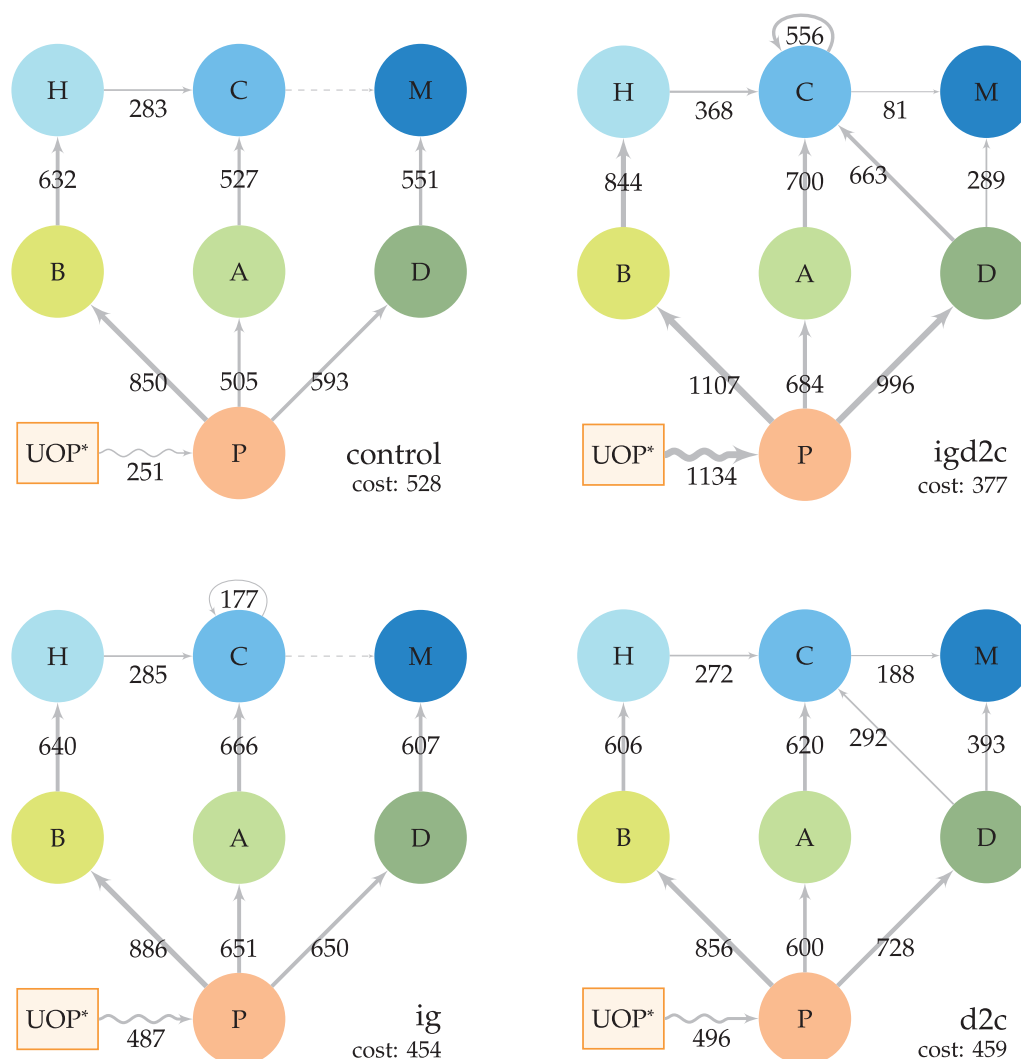
Fig. 2. Simulated nutrient and biomass fluxes (nmol P L^{-1}) between variables integrated over the course of each optimized 13-d simulation. The weight of the arrows is scaled according to the fluxes. Dashed arrows (as between ciliates [C] and mesozooplankton [M] in the *control* and *ig* configurations) have near zero fluxes and are therefore hardly realized in the optimized simulations. The wavy arrow represents remineralization of dissolved and detrital organic phosphorus (in the model explicitly resolved as UOP*). The cost function value *J* indicates the goodness-of-fit to the observational data.

and *mesh-like* food webs is clearly indicated by the maximum TL of copepods (TL$_M$) during the simulation (Table 2).

Ecosystem functioning

Both overall complexity and mesh- vs. chain-like food web structure affect ecosystem functioning (Table 2). Recycling of organic matter accumulating in the mesocosms increases by more than a factor of four between the simplest and the most complex food web. At the same time, microzooplankton productivity and primary production (NPP) by ANFs and diatoms increase. Via which group inorganic nutrients enter the plankton community depends on the food web structure. Bacteria take up the majority of the inorganic nutrients in the chain-like webs, while in the mesh-like webs an increase in nutrient uptake can occur successively, for example, from ANFs to

diatoms to bacteria. Food webs with simple and intermediate complexity result in a similarly high amount of secondary production by copepods and a high TTE, while the most complex model has notably lower copepod production and TTE.

Resolving ciliate IGP in the *igd2c* web reduces copepod productivity substantially (Table 2). This reduction coincides with halved TTE while recycling and NPP double. Such an effect of IGP is not apparent in the chain-like food webs.

Sensitivities to initial conditions and structural changes

Food web structure and certain trophic interactions, in particular IGP, determine sensitivities of projected ecosystem functions to variations in plankton composition. With different initial conditions, mesh- and chain-like food web structures remain clearly distinguishable by a different maximum

Table 2. Ecosystem functions across selected optimized simulations: NPP, NSP for copepods (mesozooplankton; M) and the microbial loop (H + C), TTE and range of the TL of M for food webs of different complexity (total no. of parameters).

Configuration	Type	Complexity	NPP	NSP$_{H+C}$	NSP$_M$	Recycling	TTE$_M$	TL$_M$
		No. of parameters	μmol CL^{-1}d^{-1}			nmol PL^{-1}d^{-1}	%	Min–max
control	"chain"	20	8.95	2.22	0.21	19.30	5.0	2.00
ig	"chain"	21	10.61	2.72	0.23	37.44	4.7	2.00
d2c	"mesh"	21	10.83	2.75	0.22	38.14	4.4	2.26–2.72
igd2c	"mesh"	22	13.70	4.82	0.14	87.71	2.2	2.20–2.59
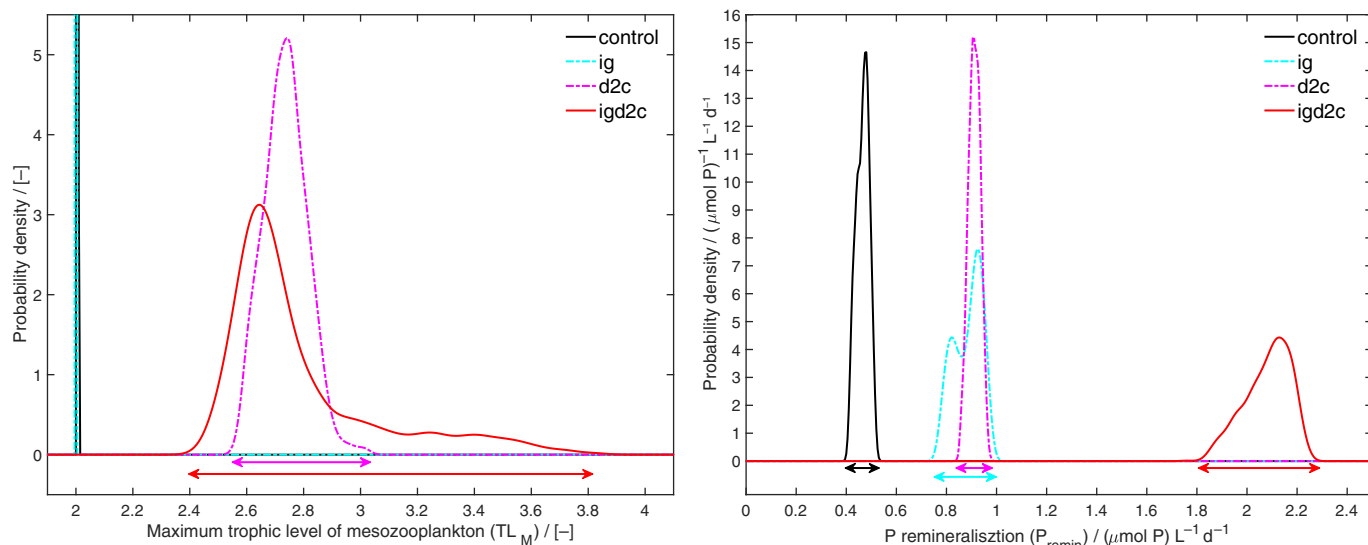
Fig. 3. Probability density functions of (left) the maximum TL of copepods (TL$_M$) and (right) remineralization of accumulating organic P (UOP*) to PO$_4^{3-}$ in ensemble simulations varying initial conditions randomly by $\pm$ 20% for selected model configurations. Chain- and mesh-like food webs are indicated by cold and warm colors, respectively.

TL of copepods (max. TL$_M$; Fig. 3). The mesh-like food webs (*d2c* and *igd2c*) exhibit a variable maximum TL$_M$, indicating a substantial degree of omnivory, while the chain-like food webs (*control* and *ig*) yield a maximum TL$_M$ close to 2 indicative of pure herbivory. Here, the spread expresses that TL$_M$ in the chain-like food webs is insensitive to variations in the relative proportions of heterotrophs and autotrophs in the initial conditions in contrast to the mesh-like food webs.

The food webs sustain their different levels of remineralization (Table 2; Fig. 3). For both chain- and mesh-like systems, adding IGP increases the level and variational range (spread) of possible remineralization. The same effect of IGP, namely increasing both level and variability, is also evident for both NPP (Supporting Information Fig. S4) and microbial loop production (NSP of H and C: NSP$_{H+C}$; Fig. 4b; cf. Supporting Information Fig. S5 for the corresponding probability density functions). In particular, NPP is far more variable than the remineralization rate. Eventually, the more complex food webs exhibit a more productive microbial loop,

but do not differ systematically in copepod production (NSP$_M$).

However, chain- and mesh-like webs differ in variability and in their reaction to including IGP (Fig. 4c). The chain-like webs react with a large spread of copepod production. In the mesh-like food webs, copepod production is notably less variable than in the chain-like webs, and decreases when considering microzooplankton IGP. This pattern is reflected in the TTE (Fig. 4a). The efficiency of trophic transfer is, however, not directly linked to the length of the food chain from primary producers to copepods, as food webs with same maximum TL can have distinctly different TTE (Fig. 3). Irrespective of food web structure, a confined maximum TL$_M$ is associated with high variability in TTE and copepod production (Figs. 3, 4), and vice versa.

The chain vs. mesh character of realized pathways in the different model configurations determines which role trophic cascades play in the simulations. The simplest chain-like food web (*control*) directly links increases in primary production to

Table 3. Sensitivity of ecosystem functions (as in Table 2), expressed as coefficient of variation (standard deviation/mean of all ensemble simulations; %) in ensemble simulations randomly varying initial conditions by $\pm$ 20% for selected food webs.

Configuration		CV (NPP)	CV (NSP$_{H+C}$)	CV (NSP$_M$)	CV (recycling)	CV (TTE$_M$)	CV (TL$_M$)
control	"chain"	16.00	9.76	29.08	5.41	19.99	0.08
ig	"chain"	19.00	10.88	39.37	6.31	26.23	0.00
d2c	"mesh"	9.31	4.41	8.37	2.54	9.31	2.78
igd2c	"mesh"	10.60	5.39	11.21	4.37	10.65	9.61
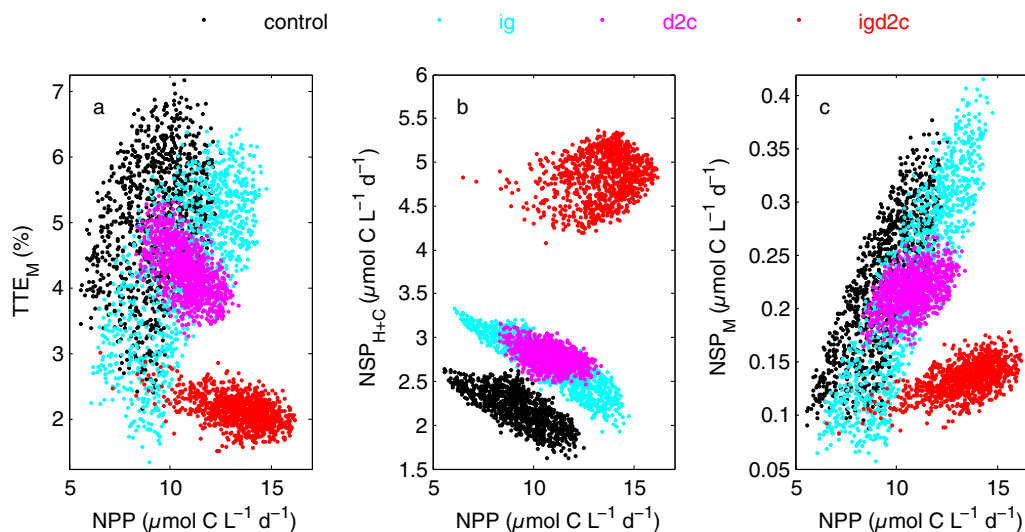
Fig. 4. Effects of randomly varying initial conditions within a $\pm$ 20% range on ecosystem functions in food webs of different complexity. Ecosystem functions are NPP vs. TTE; (**a**) from primary producers to M, NSP of the microbial loop (NSP$_{H+C}$; **b**) and of copepods (NSP$_M$; **c**).

higher copepod production (Fig. 4). The more complex mesh-like models show a weaker and more variable increase, with the weakest increase found for the most complex food webs that resolve IGP.

The variability of all ensemble simulations indicates the sensitivity of ecosystem functioning for the different food webs. The chain-like model food webs are most sensitive in terms of ecosystem functions to changes in initial values compared to the mesh-like models, indicated by the consistently higher coefficient of variation (Table 3). The only exception is the maximum TL$_M$, which designates the rigidity of trophic interactions in the chain-like models. While the lower TL functions (primary and microbial loop production, recycling) have sensitivity higher by about a factor of two, copepod production, and to a lesser degree TTE, are distinctly more sensitive in the chain-like than in the mesh-like models. Within chain- and mesh-like food webs, adding IGP increases the sensitivity of all ecosystem functions.

Discussion

The present study reveals effects of food web structure and the underlying trophic interactions on ecosystem functioning and sensitivity, starting from the established Minimum Microbial Food Web model (Thingstad et al. 2007). The strength of the approach lies in comparing models that are objectively fitted to observations and present alternative explanations for the same observations. Here, the trophic links, prescribed by the model equations, specify the models' complexity and possible pathways of mass flux. The models' best fit to observations then determines major trophic links and with it flow diversity that in turn may affect ecosystem properties like stability (Saint-Béat et al. 2015).

From parallel food chains to mesh-like food webs

The valuable PAME-I data present the opportunity to understand in detail differences in mass fluxes within different model food webs and their effects on ecosystem functioning. In general, the more complex food webs host a higher nutrient recycling capacity, which is linked to the enhanced productivity of the microzooplankton in the microbial loop. As the model assumes unassimilated organic phosphorous to originate from grazing processes, any additional trophic link supplies UOP* which ultimately fuels NPP. Which of the osmotrophs, ANFs, diatoms or bacteria, takes up the inorganic

nutrients depends on the food web structure and its inherent top-down control and is not purely bottom-up driven.

Chain-like food webs exhibit a high copepod production, which is facilitated by a high TTE of the classical herbivorous grazing food chain. In the mesh-like *d2c* food web, the same amount of copepod production is fueled by diatoms and ciliates, although TTE is comparatively lower. In these model solutions, the ciliates may benefit from higher diatom production, but with the additional TL the mass transfer to copepods becomes less efficient. When adding IGP, TTE is reduced substantially, as part of the ciliate production is consumed by ciliates and recycled rather than being transferred to the copepods. In contrast, in the chain-like solutions copepods benefit directly from the higher diatom production via the classical grazing food chain with high TTE.

Our optimized simulations demonstrate that different food webs can capture the observed dynamics equally well, ranging from complex food webs to a classical diatom–copepod food chain. The chain-like food webs disregard the hypothesis that particularly small-celled diatoms in the experiment might have been accessible to ciliates rather than only to copepods. This additional trophic link gives the double pentagon model of parallel food chains a mesh-like character and adds flexibility to the success of ciliates, which are a substantial part of the copepod diet across different marine ecosystems (Calbet and Saiz 2005). After calibration, our cost function values confirm that the *d2c* model of Larsen et al. (2015) outperforms the original chain-like food web model (*control*) for the PAME-I setup. The conceptual idea of a food web with fully separate food chains therefore seems oversimplified, given that marine food webs tend to be diverse and complex rather than linear with few dominant predators per TL (Hessen and Kaartvedt 2014).

Food web sensitivity

Food web structure has a marked effect on sensitivity of simulated ecosystem functions to changes in biological conditions. The optimized model configurations involve two scenarios: inflexible chain-like food webs where copepods rely only on diatoms and cannot feed substantially on ciliates (Supporting Information Table S5), and mesh-like food webs with a greater variety of food sources available to the top consumers. This larger choice of available food sources is indicated by the enhanced variability of the maximum TL of copepods (TL_M; Table 2; Fig. 3), which integrates the underlying food web structure. It is a valuable indicator for shifts in food web structure related to, e.g., global change (Saint-Béat et al. 2018). In mesh-like systems, this larger variety of possible pathways increases variability of remineralization more strongly than is possible in the chain-like systems. The larger variability demonstrates that a complex model food web responds less rigidly to perturbations than a simple one, and diverging changes may occur via a range of possible pathways.

At the same time, food web complexity buffers higher TL ecosystem functions like copepod production and TTE to copepods. This buffering is evident from the correlation between NPP and copepod production (Fig. 4). In the chain-like webs, an increase in NPP implies higher copepod production, as determined by the inherent classical diatom–copepod food chain. The variability around this correlation (i.e., the variable amount of NSP_M at similar levels of NPP), is linked to whether NPP is provided by diatoms or by ANFs unavailable to copepods. This balance is determined by the initial biomass of their predators, so that high ciliate and low copepod biomass (high C_0/M_0 ratio) lead to a high diatom fraction of NPP and vice versa (Fig. 5a,b). A high diatom fraction of NPP in turn implies a high TTE in chain-like food webs, where a high copepod production is linked to a low initial copepod biomass. Food webs with a mesh-like structure, in contrast, decouple TTE and copepod production from initial biomass values (Fig. 5a,c). Highest copepod production is still achieved in systems with high NPP (Fig. 4c), but productivity is no longer linked to the identity of the primary producer, and NPP is partitioned more equally between flagellates and diatoms (cf. NPP and the D fraction of NPP in Figs. 4a, 5b, respectively, for similar TTE values). Both TTE and copepod production are at the lower end of the range exhibited by the chain-like models, as more and longer pathways through the food web to copepods exist. The slightly declining TTE may dampen effects of NPP change for copepods, while the increasing TTE in chain-like webs enhances it. In mesh-like food webs, a high initial copepod biomass yields slightly higher copepod production than a low value (Fig. 5c).

Effects of adding IGP consequently depend on the food web structure. Adding IGP to chain-like food webs increases variability of NPP, microbial loop and copepod production by affecting competition between diatoms and ANFs via top-down control of ANFs. In food webs without IGP, webs with distinctly different maximum TL_M may be similarly efficient in terms of trophic transfer (cf. food webs *control* vs. *d2c*). When adding IGP to mesh-like food webs, part of the production otherwise available to copepod feeding is rerouted to remineralization instead, making trophic transfer less efficient. This decrease arises although the food chain might be shorter, as indicated by a lower maximum TL_M. In the chain-like food webs, adding IGP may decrease TTE by increasing production in the separated microbial loop, with the option of reducing diatom production through competition. IGP, as one example of omnivory in plankton communities, is therefore a decisive feature for modeling projections.

Intraguild predation

In our study, IGP expands the scope of prey, and thus the level of omnivory, for ciliates. After model calibration, our study reveals improved model fits to the observational data of the Kongsfjorden plankton ecosystem when IGP is added to the *control* (*ig*) and *d2c* (*igd2c*) models. This addition maintains
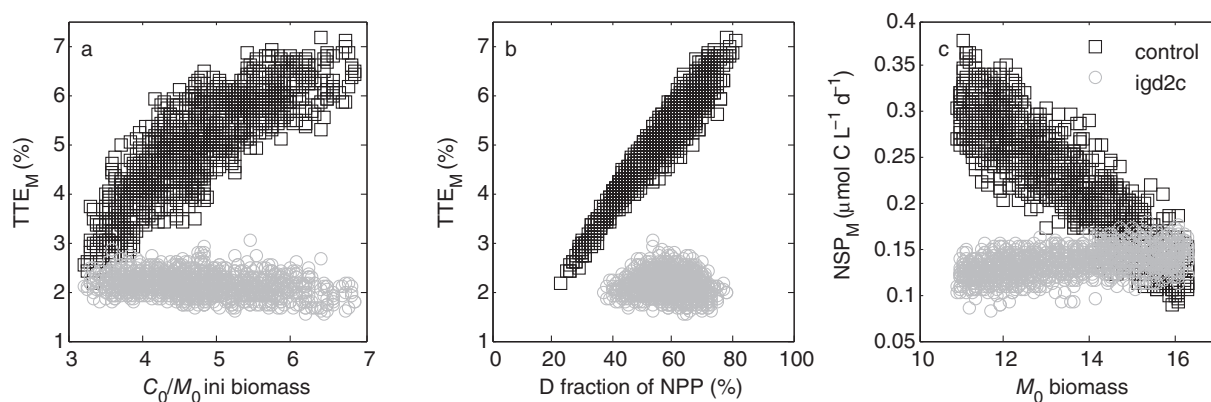
Fig. 5. TTE from autotrophs to copepods depending on (**a**) initial ciliate to copepod biomass ratio (C_0/M_0) and (**b**) diatom fraction of primary production in two simulations with chain-like (*control*) and mesh-like (*igd2c*) food web structure. (**c**) NSP of copepods (NSP_M) correlation depending on initial copepod biomass.

a statistically reasonable balance between model complexity and the improvements of model fits to the data. It is supported by evidence for defined size ranges of high predation that indicate omnivory and IGP of microzooplankton in the Fram Strait (Lampe et al. 2021), affecting both autotrophic and heterotrophic flagellates, and likewise size ranges of small ciliates and diatoms. Overall, the grazing of, for example, large tintinnids on other smaller ciliates suggests IGP to become relevant for models that treat microzooplankton as a single functional type.

Considering IGP in models will affect the representation of bottom-up and top-down controls, and its omission may severely bias a model's sensitivity to changes in community composition. Our simulations confirm that IGP slows down energy transfer to higher TLs while promoting NPP and recycling, (Table 2; Wang et al. 2019). The underlying reduction of top-down control allows different energy pathways in parallel through the food web to the top predator.

The crucial role of microzooplankton IGP has already been demonstrated when simulating dynamics in mesocosm with high levels of mixotrophic dinoflagellates (Su et al. 2018). In a size-resolved one-dimensional plankton ecosystem model, removing zooplankton IGP even compromises fish survival as small- and medium-sized zooplankton may hide from fish in deep waters without fearing predation by larger zooplankton (Castellani et al. 2013). Adding IGP might also be reasonable for heterotrophic nanoflagellates in the Minimum model (Moustaka-Gouni et al. 2016), with effects likely within the microbial (left-hand) loop.

Resolving IGP has likely been hindered by methodological challenges to obtain observations for natural communities. Reciprocal predation between similar-sized organisms, as evident for dinoflagellates and heterotrophic nanoflagellates (*see* review by Hansen et al. 1994; Moustaka-Gouni et al. 2016), is often neglected and complicates detection and quantification of IGP. Also, zooplankton feeding is often measured as bulk

net "disappearance" of similarly sized groups in bottle incubations of natural prey (Nejstgaard et al. 2001). Dilution experiments used to measure microzooplankton grazing may include several types of predators and trophic cascades (Calbet and Saiz 2013). Molecular analysis of gut content (Nejstgaard et al. 2008) has a better potential to reveal IGP, especially if including detection of prey types, for example, by metabarcoding (Ray et al. 2016; Yeh et al. 2020). Molecular analyses cannot detect cannibalism, though, and may not be sensitive enough to detect feeding on taxonomically closely related species. As limits remain, new high-resolution optical approaches might allow in situ measurements of natural communities in the future.

IGP dampens community responses to experimental environmental perturbations (Moustaka-Gouni et al. 2016) and might increase resilience to both environmental (bottom-up) and biotic (top-down) changes in model projections, as would generally be expected for more diverse food webs (Saint-Béat et al. 2015). In our simulations, IGP makes trophic transfer less sensitive to initial biomass changes and decouples TTE from food chain length. As mesozooplankton production and TTE are strong predictors of fisheries yields (Friedland et al. 2012), model projections of such ecosystem services may be affected by resolving IGP.

Trophic cascades

Trophic cascades can result in alternating shifts in the biomass of adjacent TLs (Pershing et al. 2015) and a pronounced cascading effect implies inter alia a direct strong link between TLs, effectively channeling mass and energy up the food chain.

Our results provide some hints how the role of trophic cascades and may differ between simple and complex food webs. The strong coupling of copepod production with NPP, the ciliate-copepod initial biomass ratio and (inversely) copepod initial biomass indicates the potential for dominant trophic

cascades in the chain-like food webs. These food webs incorporate a separate even-length food chain in parallel to the microbial pentagon web, and this separation will affect the long-term response to both top-down and bottom-up forcing (Wollrab and Diehl 2015). The comparatively weaker coupling between NPP and copepod production in the more complex mesh-like food webs indicates weaker trophic cascading compared to food chains (Strong 1992; Polis and Strong 1996; Schneider et al. 2012). A more complex food web was also suggested to cause damped trophic cascades in another mesocosm experiment analyzed with the original Minimum model (Pree et al. 2017). Food web complexity (hence omnivory) is seen as one cause for the weaker evidence for cascades in marine compared to freshwater systems (Hessen and Kaartvedt 2014; Pershing et al. 2015), and omnivory is common in marine food webs (Thompson et al. 2007). The prominence of trophic cascades will be highly relevant for model projections of future ecosystem changes and effects of fisheries (Bascompte et al. 2005; Frank et al. 2005; Maar et al. 2018). An oversimplified food web structure, or one with unrealistically strong links between primary and copepod production, may therefore overestimate ecosystem sensitivity and effects on fisheries (Pahl-Wostl 1997; Saint-Béat et al. 2018).

Biogeochemistry and need for observations

The present analyses imply that choosing a specific food web structure may predetermine projections of biogeochemistry to be governed either by vertical export or by rapid organic matter recycling. In the Minimum model, the dominance of vertical export of Si-ballasted detritus from diatoms and fecal pellets vs. rapid recycling in the upper ocean relates to the balance between the "classical" food chain and the microbial food web (Thingstad 2020). In our simulations, this balance is indicated by the maximum TL of copepods (near 2 in simulations with dominant food chain, higher in simulations with a strong microbial loop). Considering trophic interactions like IGP might further yield divergent biogeochemical flux estimates by promoting recycling and NPP. As sensitivities of model solutions, for example, to global change, will differ while fitting biomass observations similarly well, traditional model assessment may become considerably less conclusive.

Given the flexibility of trophic interactions in complex models, our results document the complicacy in identifying the most credible solution, which becomes invidious when only biomass observations are available. This dilemma constitutes a severe challenge for model projections of planktonic ecosystems, in particular for vulnerable regions like the Arctic. For example, a stronger retention of nutrients, by recycling in the upper ocean, may prolong growth also of large phytoplankton such as diatoms towards autumn, which are a critical food source for copepods before entering diapause in the deep ocean (Falk-Petersen et al. 2009; Pond et al. 2012). Observations revealing trophic structure and interactions, such as feeding rates (in particular for microzooplankton), δ^{15}N and

potentially eDNA, as well as a consistent focus on measuring traits (Kiørboe et al. 2018) are therefore of utmost importance.

Observations of trophic interactions are particularly relevant on the global scale, where data used to assess models, such as remote sensing estimates of NPP, may not suffice to constrain microbial ecological effects on biogeochemistry. In our simulations, "lower TL" ecosystem functions like NPP and overall recycling are notably less sensitive to changes in food web structure and trophic interactions than "upper TL" functions like TTE. Rate measurements, for example, of bacterial production, organic matter remineralization, or NH_4^+ utilization are of great importance for unambiguously identifying credible model solutions.

Nevertheless, implementing complex food webs into ocean biogeochemical general circulation models is deemed necessary for revealing effects of plankton ecology on ocean biogeochemistry. Mixotrophy is a recent example for added trophic complexity that is increasingly addressed experimentally and in modeling (Stoecker et al. 2017), with effects on ecosystem functioning such as ocean export production (Ward and Follows 2016). Adding different aspects of mixotrophy to the Minimum model, in particular regarding ciliates or the distinction between autotrophic and heterotrophic flagellates, might increase its realism, but may compromise its ability to resolve fundamental aspects of theoretical ecology (Wollrab and Diehl 2015; Våge et al. 2018; Thingstad 2020).

In general, such model approaches that consider traits and trade-offs (Banas et al. 2016; Ward and Follows 2016; Serra-Pompei et al. 2020), may yield model solutions that are more confined and may thereby help reducing uncertainties in projections of changes in plankton composition and food web structure and to assess the role of trophic complexity and flexibility for ecosystem services (A. E. F. Prowe et al., unpubl.) at times of rapid environmental change.

Conclusions

The present model simulations unravel important aspects of the role of trophic interactions and food web structure for ecosystem functioning. While different food web structures can explain observational data of nutrients and plankton biomass equally well, realized pathways of mass flux through the system may vary substantially along a complex network of potential trophic interactions, driven by trait composition and standing stocks, and may be much more variable than apparent from biomass observations.

Food web complexity in general and plankton omnivory, as analyzed here in detail for microzooplankton IGP, govern model sensitivity and ecosystem functions. IGP may increase simulated (regenerated) primary production, lower the TTE, and increase the maximum TL, depending on model structure and the complexity of trophic interactions based on the same observed plankton system. Differences are exacerbated when testing models with different initial biomass of the plankton

components, with simple food webs showing higher sensitivity, and thus larger uncertainty, than complex ones. Underrepresented trophic interactions deserve more attention and a detailed trade-off based approach in experimental and modeling studies if we are to achieve a sound understanding of future ocean ecosystems.

Data availability statement

Model data presented in this paper are available under [https://hdl.handle.net/20.500.12085/3af155c8-6301-4958-9375-9ee016565bed].

References

Banas, N. S., E. F. Møller, T. G. Nielsen, and L. B. Eisner. 2016. Copepod life strategy and population viability in response to prey timing and temperature: Testing a new model across latitude, time, and the size spectrum. Front. Mar. Sci. **3**:225. doi:10.3389/fmars.2016.00225

Bascompte, J., C. J. Melian, and E. Sala. 2005. Interaction strength combinations and the overfishing of a marine food web. Proc. Natl. Acad. Sci. USA **102**: 5443–5447. doi:10.1073/pnas.0501562102

Brun, P., K. Stamieszkin, A. W. Visser, P. Licandro, M. R. Payne, and T. Kiørboe. 2019. Climate change has altered zooplankton-fuelled carbon export in the North Atlantic. Nat. Ecol. Evol. **3**: 416. doi:10.1038/s41559-018-0780-3

Calbet, A., and E. Saiz. 2005. The ciliate-copepod link in marine ecosystems. Aquat. Microb. Ecol. **38**: 157–167.

Calbet, A., and E. Saiz. 2013. Effects of trophic cascades in dilution grazing experiments: From artificial saturated feeding responses to positive slopes. J. Plankton Res. **35**: 1183–1191. doi:10.1093/plankt/fbt067

Castellani, M., R. Rosland, A. Urtizberea, and O. Fiksen. 2013. A mass-balanced pelagic ecosystem model with size-structured behaviourally adaptive zooplankton and fish. Ecol. Model. **251**: 54–63. doi:10.1016/j.ecolmodel.2012.12.007

Diehl, S., and M. Feissel. 2001. Intraguild prey suffer from enrichment of their resources: A microcosm experiment with ciliates. Ecology **82**: 2977–2983.

Dobson, A., and others. 2006. Habitat loss, trophic collapse, and the decline of ecosystem services. Ecology **87**: 1915–1924.

Dolan, J. R., and D. W. Coats. 1991. A study of feeding in predacious ciliates using prey ciliates labeled with fluorescent microspheres. J. Plankton Res. **13**: 609–627.

Dufour, K., F. Maps, S. Plourde, P. Joly, and F. Cyr. 2016. Impacts of intraguild predation on Arctic copepod communities. Front. Mar. Sci. **3**:185. doi:10.3389/fmars.2016.00185

Falk-Petersen, S., P. Mayzaud, G. Kattner, and J. R. Sargent. 2009. Lipids and life strategy of Arctic *Calanus*. Mar. Biol. Res. **5**: 18–39. doi:10.1080/17451000802512267

Frank, K. T., B. Petrie, J. S. Choi, and W. C. Leggett. 2005. Trophic cascades in a formerly cod-dominated ecosystem. Science **308**: 1621–1623. doi:10.1126/science.1113075

Franzé, G., and M. Modigh. 2013. Experimental evidence for internal predation in microzooplankton communities. Mar. Biol. **160**: 3103–3112. doi:10.1007/s00227-013-2298-1

Friedland, K. D., and others. 2012. Pathways between primary production and fisheries yields of large marine ecosystems. PLoS One **7**: e28945. doi:10.1371/journal.pone.0028945

Hansen, B., P. K. Bjørnsen, and P. J. Hansen. 1994. The size ratio between planktonic predators and their prey. Limnol. Oceanogr. **39**: 395–403.

Hansen, N., and A. Ostermeier. 2001. Completely derandomized self-adaptation in evolution strategies. Evol. Comput. **9**: 159–195.

Hessen, D. O., and S. Kaartvedt. 2014. Top-down cascades in lakes and oceans: Different perspectives but same story? J. Plankton Res. **36**: 914–924. doi:10.1093/plankt/fbu040

Holt, R. D., and G. A. Polis. 1997. A theoretical framework for intraguild predation. Am. Nat. **149**: 745–764.

Kiørboe, T., A. P. Visser, and K. H. Andersen. 2018. A trait-based approach to ocean ecology. Ices J. Mar. Sci. **75**: 1849–1863. doi:10.1093/icesjms/fsy090

Kuppardt-Kirmse, A., and A. Chatzinotas. 2020. Intraguild predation: Predatory networks at the microbial scale. Springer. doi:10.1007/978-3-030-45599-6_3

Lampe, V., E.-M. Nöthig, and M. Schartau. 2021. Spatio-temporal variations in community size structure of Arctic protist plankton in the Fram Strait. Front. Mar. Sci. **7**: 579880. doi:10.3389/fmars.2020.579880

Larsen, A., J. K. Egge, J. C. Nejstgaard, I. Di Capua, R. Thyrhaug, G. Bratbak, and T. F. Thingstad. 2015. Contrasting response to nutrient manipulation in Arctic mesocosms are reproduced by a minimum microbial food web model. Limnol. Oceanogr. **60**: 360–374. doi:10.1002/lno.10025

Li, W. K. W., F. A. McLaughlin, C. Lovejoy, and E. C. Carmack. 2009. Smallest algae thrive as the Arctic Ocean freshens. Science **326**: 539–539. doi:10.1126/science.1179798

Löder, M. G. J., M. Boersma, A. C. Kraberg, N. Aberle, and K. H. Wiltshire. 2014. Microbial predators promote their competitors: Commensalism within an intra-guild predation system in microzooplankton. Ecosphere **5**: art128. doi:10.1890/ES14-00037.1

Maar, M., and others. 2018. Responses of summer phytoplankton biomass to changes in top-down forcing: Insights from comparative modelling. Ecol. Model. **376**: 54–67. doi:10.1016/j.ecolmodel.2018.03.003

McGinty, N., A. D. Barton, N. R. Record, Z. V. Finkel, D. G. Johns, C. A. Stock, and A. J. Irwin. 2021. Anthropogenic climate change impacts on copepod trait biogeography. Glob. Chang. Biol. **27**: 1431–1442. doi:10.1111/gcb.15499

Moustaka-Gouni, M., K. A. Kormas, M. Scotti, E. Vardaka, and U. Sommer. 2016. Warming and acidification effects on

planktonic heterotrophic pico- and nanoflagellates in a mesocosm experiment. Protist **167**: 389–410. doi:10.1016/j.protis.2016.06.004

Nejstgaard, J. C., M. E. Frischer, P. Simonelli, C. Troedsson, M. Brakel, F. Adiyaman, A. F. Sazhin, and L. F. Artigas. 2008. Quantitative PCR to estimate copepod feeding. Mar. Biol. **153**: 565–577. doi:10.1007/s00227-007-0830-x

Nejstgaard, J. C., L. J. Naustvoll, and A. Sazhin. 2001. Correcting for underestimation of microzooplankton grazing in bottle incubation experiments with mesozooplankton. Mar. Ecol. Prog. Ser. **221**: 59–75.

Pahl-Wostl, C. 1997. Dynamic structure of a food web model: Comparison with a food chain model. Ecol. Model. **100**: 103–123. doi:10.1016/S0304-3800(97)00151-8

Pershing, A. J., and others. 2015. Evaluating trophic cascades as drivers of regime shifts in different ocean ecosystems. Philos. Trans. Roy. Soc. B Biol. Sci. **370**: 20130265. doi:10.1098/rstb.2013.0265

Polis, G. A., and D. R. Strong. 1996. Food web complexity and community dynamics. Am. Nat. **147**: 813–846.

Pond, D. W., G. A. Tarling, P. Ward, and D. J. Mayor. 2012. Wax ester composition influences the diapause patterns in the copepod *Calanoides acutus*. Deep Sea Res. Part Ii Topic. Stud. Oceanogr. **59**: 93–104. doi:10.1016/j.dsr2.2011.05.009

Pree, B., and others. 2017. Dampened copepod-mediated trophic cascades in a microzooplankton-dominated microbial food web: A mesocosm study. Limnol. Oceanogr. **62**: 1031–1044. doi:10.1002/lno.10483

Ray, J. L., and others. 2016. Metabarcoding and metabolome analyses of copepod grazing reveal feeding preference and linkage to metabolite classes in dynamic microbial plankton communities. Mol. Ecol. **25**: 5585–5602. doi:10.1111/mec.13844

Saint-Béat, B., and others. 2015. Trophic networks: How do theories link ecosystem structure and functioning to stability properties? A review. Ecol. Indic. **52**: 458–471. doi:10.1016/j.ecolind.2014.12.017

Saint-Béat, B., F. Maps, and M. Babin. 2018. Unraveling the intricate dynamics of planktonic Arctic marine food webs. A sensitivity analysis of a well-documented food web model. Prog. Oceanogr. **160**: 167–185. doi:10.1016/j.pocean.2018.01.003

Schartau, M., and others. 2017. Reviews and syntheses: Parameter identification in marine planktonic ecosystem modelling. Biogeosciences **14**: 1647–1701. doi:10.5194/bg-14-1647-2017

Schneider, F. D., S. Scheu, and U. Brose. 2012. Body mass constraints on feeding rates determine the consequences of predator loss. Ecol. Lett. **15**: 436–443. doi:10.1111/j.1461-0248.2012.01750.x

Serra-Pompei, C., F. Soudijn, A. W. Visser, T. Kiørboe, and K. H. Andersen. 2020. A general size-and trait-based model of plankton communities. Prog. Oceanogr. **189**: 102473.

Søreide, J. E., E. Leu, J. Berge, M. Graeve, and S. Falk-Petersen. 2010. Timing of blooms, algal food quality and *Calanus glacialis* reproduction and growth in a changing Arctic. Glob. Chang. Biol. **16**: 3154–3163. doi:10.1111/j.1365-2486.2010.02175.x

Steinberg, D. K., and M. R. Landry. 2017. Zooplankton and the ocean carbon cycle. Ann. Rev. Mar. Sci. **9**: 413–444. doi:10.1146/annurev-marine-010814-015924

Stoecker, D. K., P. J. Hansen, D. A. Caron, and A. Mitra. 2017. Mixotrophy in the marine plankton. Ann. Rev. Mar. Sci. **9**: 311–335. doi:10.1146/annurev-marine-010816-060617

Strong, D. R. 1992. Are trophic cascades all wet - differentiation and donor-control in speciose ecosystems. Ecology **73**: 747–754.

Su, B., M. Pahlow, and A. E. F. Prowe. 2018. The role of microzooplankton trophic interactions in modelling a suite of mesocosm ecosystems. Ecol. Model. **368**: 169–179. doi:10.1016/j.ecolmodel.2017.11.013

Thingstad, T. F. 2020. How trophic cascades and photic zone nutrient content interact to generate basin-scale differences in the microbial food web. Ices J. Mar. Sci. **77**: 1639–1647. doi:10.1093/icesjms/fsaa028

Thingstad, T. F., and others. 2007. Ability of a "minimum" microbial food web model to reproduce response patterns observed in mesocosms manipulated with N and P, glucose, and Si. J. Mar. Syst. **64**: 15–34. doi:10.1016/j.jmarsys.2006.02.009

Thompson, R. M., M. Hemberg, B. M. Starzomski, and J. B. Shurin. 2007. Trophic levels and trophic tangles: The prevalence of omnivory in real food webs. Ecology **88**: 612–617.

Våge, S., and others. 2018. Simple models combining competition, defence and resource availability have broad implications in pelagic microbial food webs. Ecol. Lett. **21**: 1440–1452. doi:10.1111/ele.13122

Vasseur, D. A., and J. W. Fox. 2009. Phase-locking and environmental fluctuations generate synchrony in a predator–prey community. Nature **460**: 1007–1010. doi:10.1038/nature08208

Wang, S., U. Brose, and D. Gravel. 2019. Intraguild predation enhances biodiversity and functioning in complex food webs. Ecology **100**: e02616. doi:10.1002/ecy.2616

Ward, B. A., and M. J. Follows. 2016. Marine mixotrophy increases trophic transfer efficiency, mean organism size, and vertical carbon flux. Proc. Natl. Acad. Sci. USA **113**: 2958–2963. doi:10.1073/pnas.1517118113

Ward, B. A., M. Schartau, A. Oschlies, A. P. Martin, M. J. Follows, and T. R. Anderson. 2013. When is a biogeochemical model too complex? Objective model reduction and selection for North Atlantic time-series sites. Prog. Oceanogr. **116**: 49–65. doi:10.1016/j.pocean.2013.06.002

Wollrab, S., and S. Diehl. 2015. Bottom-up responses of the lower oceanic food web are sensitive to copepod mortality and feeding behavior. Limnol. Oceanogr. **60**: 641–656. doi:10.1002/lno.10044

Yang, J., M. G. J. Löder, K. H. Wiltshire, and D. J. S. Montagnes. 2021. Comparing the trophic impact of microzooplankton during the spring and autumn blooms in temperate waters. Estuar. Coast. **44**: 189–198. doi:10. 1007/s12237-020-00775-4

Yeh, H., J. Questel, K. Maas, and A. Bucklin. 2020. Metabarcoding analysis of regional variation in gut contents of the copepod *Calanus finmarchicus* in the North Atlantic Ocean. Deep-Sea Res. **II**: 104738.

Conflict of Interest

None declared.